*Korean J. Chem. Eng.*, **29**(12), 1722-1729 (2012)
DOI: 10.1007/s11814-012-0076-2

# Photocatalytic degradation of azo dye using $TiO_2$ supported on spherical activated carbon

**Ji-Won Yoon*, Mi-Hwa Baek*, Ji-Sook Hong*, Chang-Yong Lee**, and Jeong-Kwon Suh*,†**

*Research Center for Environmental Resources & Processes, Korea Research Institute of Chemical Technology, Daejeon 305-600, Korea
**Department of Environmental Engineering, Kongju National University, Chungnam 314-701, Korea
(*Received 31 January 2012 • accepted 24 May 2012*)

**Abstract**−$TiO_2$ supported on spherical activated carbon ($TiO_2$/SAC) was prepared through an ion-exchange method followed by a heat-treatment process. The adsorption characteristic of $TiO_2$/SAC was evaluated using azo dye methyl orange (MO) as a target substance, and the photocatalytic degradation of MO under UV irradiation was also discussed. A synergistic effect of both the adsorption capacity of activated carbon and the photoactivity of $TiO_2$ on the removal of MO from aqueous solution was observed. Experimental results revealed that the photocatalytic degradation of MO improved with increasing photocatalyst dosage and followed a pseudo-first order kinetic. After five-cycle runs, $TiO_2$/SAC still exhibited relatively high photocatalytic characteristic for the degradation of MO. Besides, the prepared $TiO_2$/SAC can be helpful in the easy separation of photocatalyst from solution after photocatalysis of MO. Furthermore, the use of liquid chromatography/mass spectrometry (LC/MS) technique, identified three intermediates as degradation products during the photocatalytic reaction of MO with $TiO_2$/SAC.

Key words: Titanium Dioxide, Photocatalytic Degradation, Spherical Activated Carbon, Azo Dye, Methyl Orange

## INTRODUCTION

About 15% of dyes are lost during the dyeing process which is released into the environment as industrial wastewater [1,2]. The textile effluents are deeply colored, unattractive and affect aquatic life by blocking sunlight penetration, which in turn significantly decreases the amount of dissolved oxygen [3]. Approximately 70% of azo dyes, which contain one or more azo bond (-N=N-), are widely used in the textile, paint, plastic, foodstuff, and cosmetic industries [3-6]. Some azo dyes are toxic, even mutagenic to organisms, and known to have potential carcinogens and thus may cause direct destruction of aquatic communities [7-9]. Therefore, it is highly imperative that textile effluents containing dyes be treated prior to their discharge into water bodies.

Photocatalysis has been extensively studied for the purification of contaminated water and air [10,11]. The process is one of the advanced oxidation processes that can decompose pollutants in the presence of semiconductor catalyst and UV illumination without adding oxidation agent. Among various semiconductor materials, $TiO_2$ has been widely used in photocatalysis due to its non-toxicity, affordability, high activity and relatively high chemical stability [10-12]. $TiO_2$ powder used in conventional photocatalytic reaction results in high photocatalytic performance due to its large surface area and high degree of dispersion in reaction media, but there are difficulties in recycling and reuse of $TiO_2$ powder [9,12-17]. To overcome this problem, recent studies have focused on the immobilization of the catalysts on certain supporting materials, especially, activated carbon [16-19]. Generally, the traditional methods for preparing the supported catalysts are impregnation, precipitation, and sol-gel, etc [20,21]. In our previous study [22], $TiO_2$ supported on spherical activated carbon was prepared by methods such as powder coating, sol-gel, and impregnation method. We found that photocatalyst was exfoliated and also eluted in water after 24 h. On the other hand, $TiO_2$/SAC prepared through the ion-exchange method and activation process could immobilize titanium ion without a binder and had spherical shape with smooth surface. The smooth surface can prevent problems of surface abrasion by inter-particle collision in floating photocatalytic application. Moreover, $TiO_2$/SAC, which has spherical shape, can be removed from the solution without a special separation process after photocatalytic reaction, and leaching of titanium during long-term water treatment did not occur. The development of semiconductor photocatalyst supported on spherical activated carbon, and the photocatalytic for degradation of humic acid and phenol as organic pollutants in a fluidized bed photoreactor have been reported [22-28].

In this study, $TiO_2$ supported on spherical activated carbon was prepared using the ion-exchange method and heat-treatment process by following our previous studies. The adsorbability and photocatalytic activity of $TiO_2$/SAC was evaluated by the adsorption and photocatalytic degradation of methyl orange (MO), which is one of the azo dyes mostly constituting textile effluents. The effects of photocatalyst dosage and light source on the photocatalytic activity of $TiO_2$/SAC were studied and kinetics of the degradation of MO was also analyzed. The stability of the photocatalyst was investigated through repeated use of $TiO_2$/SAC. Furthermore, the degradation products of MO were identified by LC/MS analysis.

## EXPERIMENTAL SECTION

### 1. Preparation and Characterization of $TiO_2$/SAC

$TiO_2$/SAC was prepared via the ion-exchange method and heat-treatment process as described in previous studies [27,28]. Titanium trichloride ($TiCl_3$, 20%, Kanto Chemical) and double-dis-

†To whom correspondence should be addressed.
E-mail: jksuh@krict.re.kr

tilled water with a weight ratio of $TiCl_3 : H_2O$=1 : 30 were mixed while being stirred for 10 min. Strong acid ion-exchange resin (Diaion SK1BH, Samyang Co., Ltd.) was added to $TiCl_3$ solution, and was continuously stirred at 150 rpm for 1 h at room temperature. The product was rinsed many times and then dried at 100 °C for 10 h. The dried product was heated using a tube furnace to convert it to a carbonaceous porous material. The product was stabilized under atmospheric condition at a heating rate of 1 °C/min up to 300 °C and was held for 5 h. The stabilized sample was carbonized at 700 °C for 10 min under a nitrogen flow of 2 L/min and then activated under a nitrogen/steam at 900 °C for 30 min. The heating rate was 3 °C/min up to 700 °C and then 1 °C/min up to the final temperature. $TiO_2$ content was calculated to be 10 wt% [28].

The surface morphology and size of $TiO_2$/SAC was examined by scanning electron microscopy (SEM, JSM-6700F, JEOL), and also chemical composition of $TiO_2$/SAC was analyzed by energy-dispersive X-ray spectroscopy (EDS, Bruker Quantax 200). To identify the crystalline phase of titanium in $TiO_2$/SAC, X-ray diffraction analysis was carried out using a X-ray diffractometer (XRD, D/MAX-IIIB, Rigaku) over the range $2\theta$ from 20° to 80°, with a scanning speed of 5°/min. The specific surface area of $TiO_2$/SAC was determined by Brunauer-Emmet-Teller method using Micromeritics ASAP 2010.

**2. Adsorption and Photocatalytic Activity**

Azo dye methyl orange (MO, $C_{14}H_{14}N_3O_3SNa$, MW=327.33 g/mol) selected as a target substance was purchased from Aldrich and used without any other pre-treatment. The stock solution of 1,000 mg/L was prepared in double distilled water, stored in a refrigerator at 4 °C in the dark to prevent degradation of MO by natural light, and used within one month after preparation.

Batch experiments for degradation of MO were performed in a fluidized bed photoreactor, which was made of stainless steel (10 cm diameter, 40 cm height, and 2 L capacity). Low pressure mercury lamp (UV-C, $\lambda_{max}$=254 nm) and black light blue lamp (UV-A, $\lambda_{max}$=365 nm) used as light sources were placed in the middle of the photoreactor. Air was bubbled to reaction solution through the bottom of the reactor with an air flow of 1 L/min. Adsorption experiments were conducted by adding different photocatalyst dosage (5-40 g/L) with initial MO concentration of 50 mg/L. Photocatalytic activity was evaluated under UV irradiation after stirring in the dark for 3 h to reach an adsorption-desorption equilibrium. At this time, the concentration of MO was noted $C_o$. Every sample was taken out at regular time intervals. The absorbance of the solution was measured by UV-vis spectrophotometer (Qvis 4000, Cmac) at a wavelength of 468 nm, corresponding to the maximum absorption wavelength of MO. The concentration of MO was calculated by a calibration curve. The correlation coefficient for calibration curve assessed by using MO standard solution of 5, 10, 25, 50, 100 mg/L concentration was 0.996. Mineralization (TOC removal) of MO was monitored by determining total organic carbon (TOC) concentration with TOC analyzer (Torch, Teledyne Tekmar). The calibration plot for standard solution of known TOC concentration had a correlation coefficient of 0.999. All measurements of the absorbance and TOC of the sample for each experiment were done in triplicate. The relative standard deviation (RSD) of the measured values was around 0.3-4.5%. For comparison with commercially available $TiO_2$, Deggusa P25 was chosen for the photocatalytic reaction. After photocatalytic reaction using Deggusa P25 $TiO_2$, collected samples were centrifuged at 13,000 rpm for 30 min to separate P25 $TiO_2$ particles from MO solution before analysis. The reactions were carried out at natural pH and temperature conditions. The degradation ratio (%) of MO was calculated by Eq. (1), where D is degradation ratio, $C_0$ and $C_t$ are the equilibrium concentration after adsorption and the remaining concentration of MO at certain time, respectively.

$$D(\%) = \frac{C_0 - C_t}{C_0} \times 100 \quad (1)$$

**3. LC/MS Analysis**

To identify degradation products, the samples before and after photocatalytic reaction were analyzed by liquid chromatography (LC, Hewlett Packard 1100 Series) with mass selective detector. Extend C18 column (4.6 mm×150 mm×3.5 μm) was used for separation of sample. The detection system was 1100 UV-vis diode array detector (Agilent, USA). The mobile phase was acetonitrile : 10 mM ammonium acetate (30 : 70, v/v) at a flow rate of 0.4 mL/min, and samples of 20 μl was injected. Mass analysis in the negative ions mode was performed on a mass spectrometer equipped with electrospray ionization (ESI). The minimum detection limit was in the range of a few tens to a few hundreds of ppb level.

## RESULTS AND DISCUSSION

**1. Characterization of $TiO_2$/SAC**

The specific surface area of $TiO_2$/SAC was found to be 458 $m^2$/g by using the nitrogen adsorption-desorption method. Fig. 1 shows SEM image and the result of EDS analysis for $TiO_2$/SAC. $TiO_2$/SAC showed spherical shape with smooth surface, and the diameter observed under SEM was in the range of 0.37-0.59 mm. From the EDS analysis, Ti element in $TiO_2$/SAC was confirmed.

XRD was analyzed to determine crystalline structure of titanium immobilized on spherical activated carbon. The strong peak at $2\theta$=25.4° and small peaks at $2\theta$=37.8°, 48.0°, 54.1°, 62.8°, 70.0°, and 75.0° corresponding to (101), (004), (200), (105), (211), (204), (116), (220), and (215), respectively, indicate $TiO_2$ anatase phase [5]. The peaks at $2\theta$ of 27.5°, 36.1°, 41.3°, and 56.1° which correspond to (110), (101), (111), and (220), respectively, indicate the presence of the rutile phase in $TiO_2$/SAC [5]. The XRD result showed that the titanium immobilized on spherical activated carbon existed as titanium dioxide of mixture of anatase and rutile. The relative content of anatase and rutile was determined by Spurr-Myers equation [5,29].

$$A(\%) = \frac{I_A}{I_R + 1.265 I_R} \times 100 \quad (2)$$

Where, A(%) is the relative content of anatase, $I_A$ and $I_R$ are the intensities of the anatase (101) peak at $2\theta$=25.4° and the rutile (110) peak at $2\theta$=27.5°, respectively. The phase composition obtained by above equation was 81.8% anatase and 18.2% rutile, which is very close to commercial P25 $TiO_2$ (anatase : rutile=8 : 2) and possesses very high photocatalytic activity [5]. Thus, it can be said that $TiO_2$/SAC may show high photocatalytic activity.

**2. Adsorption of MO on $TiO_2$/SAC**

Adsorption of MO on $TiO_2$/SAC is important in determining the photocatalytic degradation of MO [30]. To evaluate the adsorption

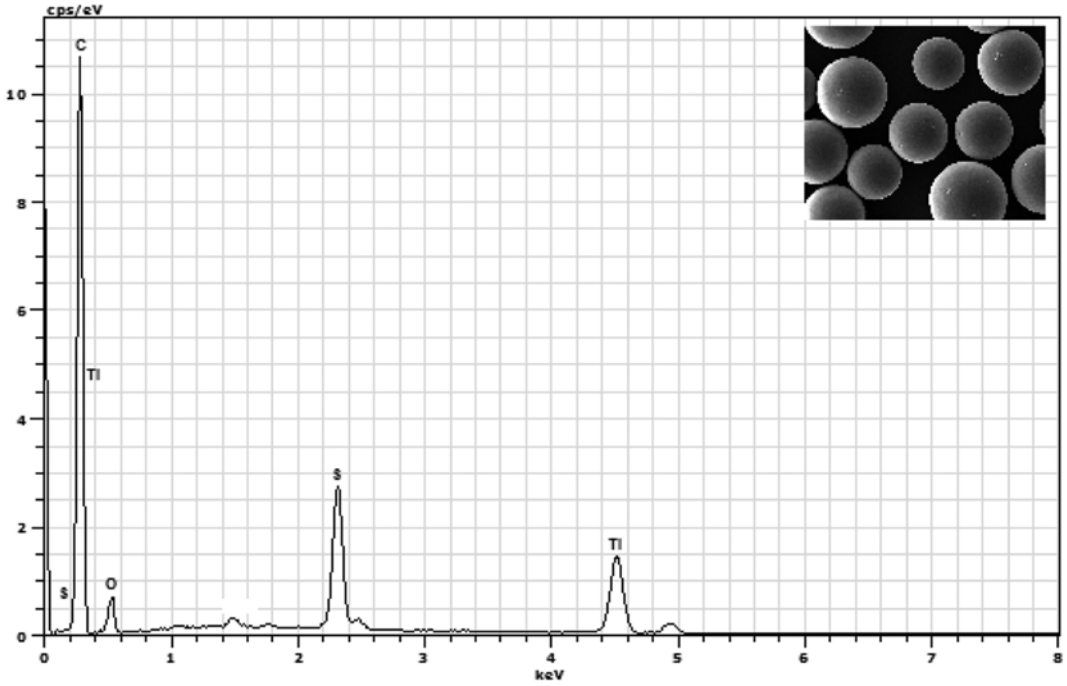


**Fig. 1. EDS spectrum and SEM image of $TiO_2$/SAC.**

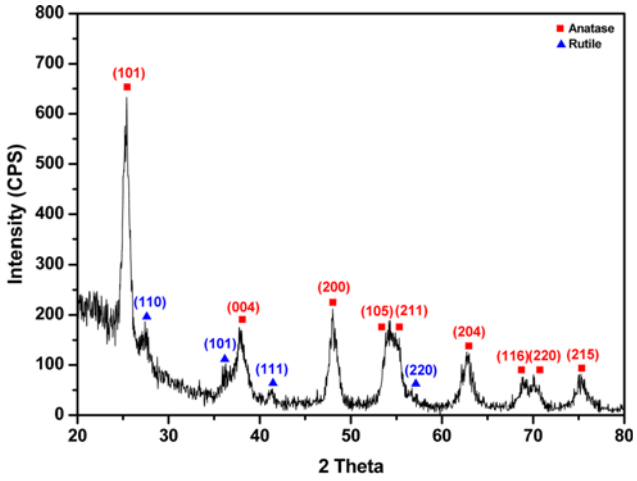


**Fig. 2. X-ray diffraction pattern of $TiO_2$/SAC.**

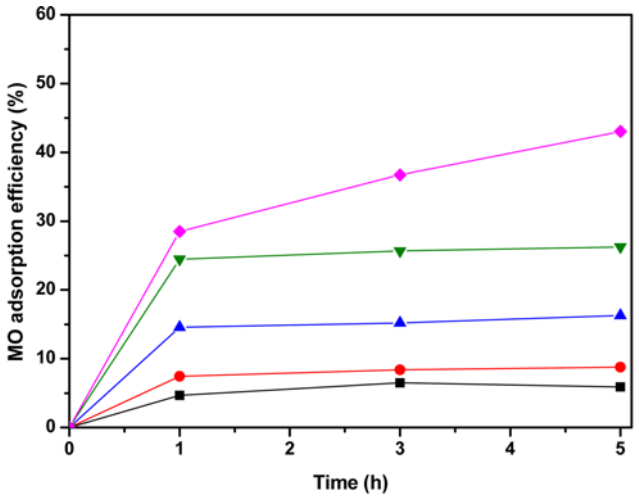


**Fig. 3. Adsorption kinetics of MO on $TiO_2$/SAC according to different photocatalyst dosage; (■) 5 g/L, (●) 10 g/L, (▲) 20 g/L, (▼) 30 g/L, (◆) 40 g/L (MO initial concentration: 50 mg/L, pH 5.7).**

equilibrium with the adsorption capacity of $TiO_2$/SAC, adsorption kinetics was carried out in the dark, varying photocatalyst dosage from 5 to 40 g/L (Fig. 3). It was found that MO adsorption on $TiO_2$/SAC quickly occurred within 1 h and reached almost equilibrium in about 3 h in the range of 5-30 g/L photocatalyst dosage. But, when photocatalyst dosage was 40 g/L, the adsorption of MO continuously increased with increasing reaction time; in other words, adsorption equilibrium was not achieved within 3 h. As shown in Fig. 3, the adsorption of MO increased with increase in photocatalyst dosage. Increasing the catalyst dosage makes a large number of sites available for a fixed concentration of MO, hence the increase in extent of adsorption [3]. MO adsorption on $TiO_2$/SAC can affect photocatalysis. Thus, photocatalyst dosage of 10 g/L, 20 g/L, and 30 g/L, which adsorption equilibrium was achieved within 3 h, was chosen for evaluation of the photocatalytic activity. To eliminate the influence of adsorption, a photocatalytic experiment was carried out after adsorption reaction of 3 h.

## 3. Photocatalytic Activity

### 3-1. Effect of $TiO_2$/SAC Dosage

Photocatalyst dosage is one of the important factors for the degradation efficiency because excessive photocatalyst dosage may reduce photocatalytic efficiency by blocking UV irradiation [19,31]. Previous researches have investigated the influence of catalyst dosage on photocatalytic degradation of target substance [4,5,19,31-35]. Sun et al. [19] reported that the increase of the photocatalyst dosage beyond the optimum value (12.5 g/L) had negative effect on the

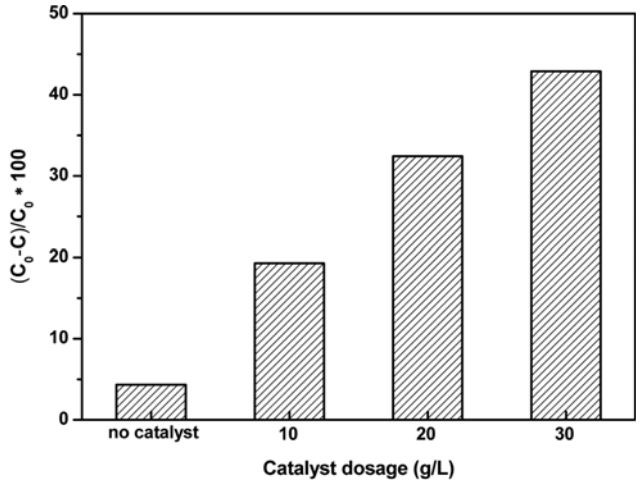


**Fig. 4. Effect of photocatalyst dosage on the photocatalytic degradation of MO. Note: $C_0$ denotes the equilibrium concentration of MO after adsorption in the dark (MO initial concentration: 50 mg/L, pH 5.7, light source: UV-C lamp, irradiation time: 7 h).**

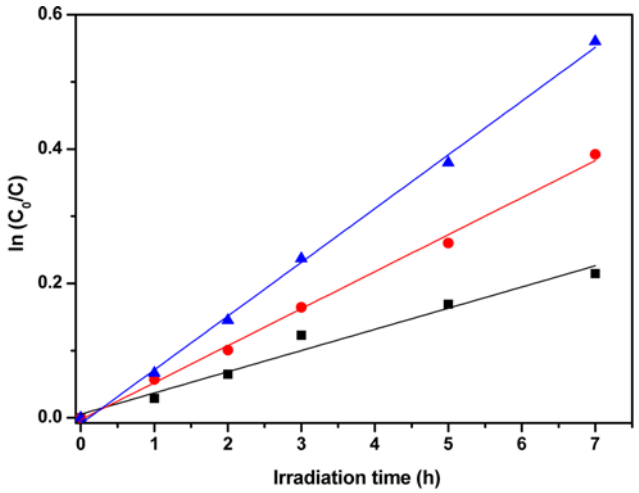


**Fig. 5. Kinetics of the degradation of MO at different photocatalyst dosage; (■) 10 g/L: $k_{app}$=0.0316 $h^{-1}$, (●) 20 g/L: $k_{app}$= 0.0551 $h^{-1}$, (▲) 30 g/L: $k_{app}$=0.0801 $h^{-1}$ (MO initial concentration: 50 mg/L, pH 5.7, light source: UV-C lamp).**

degradation efficiency of Orange G using nano-sized Sn(IV)/$TiO_2$/AC. Huang et al. [31], in their work of photocatalytic degradation of MO on Pt-$TiO_2$/zeolite, reported that the decolorization rate of MO solution decreased with any further increase in photocatalyst dosage due to light scattering and screening effect. According to the reported literature, the optimum dosage exists for a given target pollutant substance concentration [31,32]. Based on the adsorption results in the previous section, photocatalytic experiments were conducted with varying photocatalyst dosage of 10 g/L to 30 g/L to determine the effect of photocatalyst dosage. As shown in Fig. 4, the degradation of MO under UV irradiation for 7 h without photocatalyst was only 4%, suggesting that the degradation of MO by UV and air is negligible. The degradation efficiency of MO increased with increasing photocatalyst dosage from 10 g/L to 30 g/L. Increasing of photocatalyst dosage contributed to increased number of active sites on the photocatalyst surface, thereby resulting in an increase of MO degradation efficiency [3,4,19]. It could be said that the screening effect mentioned in earlier reports [31,33,34] did not show in this work condition. The kinetics of MO degradation by $TiO_2$/SAC was analyzed using the pseudo-first order model expressed in Eq. (3) [1,2,5]:

$$\ln\frac{[MO]_0}{[MO]_t} = kt \quad (3)$$

where, $[MO]_0$ is equilibrium concentration of MO after adsorption in the dark, $[MO]_t$ is remaining concentration of MO at irradiation time t, k is rate constant of pseudo-first order, and t is irradiation time. Fig. 5 is the plots of $\ln([MO]_0/[MO]_t)$ versus t. All the curves showed good linear correlation ($R^2$>0.98), suggesting that the degradation of MO by $TiO_2$/SAC follows a pseudo-first order kinetic. This is in agreement with previous literature results. It was reported that the kinetics of the photocatalytic degradation of MO by Zn(0) assisted with silica gel, mesoporous-assembled $TiO_2$ and $TiO_2$/AC followed the pseudo first-order kinetic [4], [5], and [21]. As shown in Fig. 5, the k obtained from slope of the plot increased with increasing photocatalyst dosage. Thus, it can be concluded that 30 g/L was the suitable photocatalyst dosage in this work.

3-2. Long Term Test and Influence of Light Source

To determine maximum degradation efficiency of MO by $TiO_2$/SAC, photocatalytic degradation experiment under UV irradiation for 48 h was performed with photocatalyst dosage of 30 g/L, MO concentration of 50 mg/L. The degradation efficiency of MO increased up to 98% for irradiation time of 30 h. Above this duration, degradation efficiency was almost constant. The result on the degradation efficiency of MO during irradiation time of 24 h is presented in Fig. 6. To compare the prepared $TiO_2$/SAC with commercial $TiO_2$, a photocatalytic experiment was conducted for 50 mg/L MO using P25 $TiO_2$ of 3 g/L. It was observed that degradation efficiency of MO was about 98% after UV irradiation for 5 h (figure not shown here). The photocatalytic degradation rate of MO by $TiO_2$/SAC was not as fast as that of P25 $TiO_2$ due to mass transfer limita-

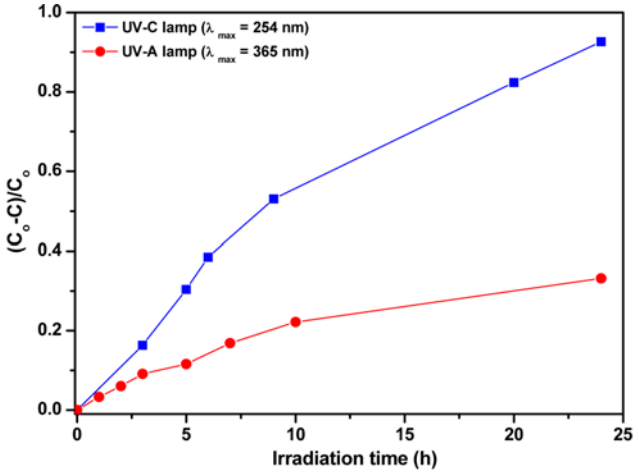


**Fig. 6. Influence of light source on the photocatalytic degradation of MO by $TiO_2$/SAC (MO initial concentration: 50 mg/L, photocatalyst dosage: 30 g/L, pH 5.7).**

tion of immobilized systems [36]. However, powder type as P25 $TiO_2$ requires an additional process step for separation of photocatalyst from treated water after photocatalysis. On the other hand, $TiO_2$/SAC used in this study is free from a separation process. Moreover, $TiO_2$/SAC has synergistic effect based on the adsorption capacity of activated carbon and the photoactivity of $TiO_2$. It has been reported that $TiO_2$-AC mixtures/composites show enhanced photocatalytic activity more than $TiO_2$ alone [17,21,37,38]. Li et al. [38] prepared $TiO_2$-coated activated carbon ($TiO_2$/AC) composites and pure $TiO_2$ powder by a sol-gel method and found that the photoactivity of $TiO_2$/AC composites is increased in methylene blue photocatalytic course more than of pure $TiO_2$ powder.

In previously reported studies, a lamp with a wavelength of 365 nm as a light source was provided for the photocatalytic degradation of MO [12,16,17,39,40]. In the present study, UV-A (315-400 nm) and UV-C (100-280 nm) lamp were used to evaluate the influence of light source on degradation of MO by $TiO_2$/SAC (Fig. 6). When using UV-A lamp, the degradation efficiency of MO was 30% during UV irradiation for 24 h. This is significantly less compared to when UV-C lamp is employed. $TiO_2$/SAC exhibited high photocatalytic activity in the wavelength range of 100-280 nm; therefore, all experiments were conducted using a UV-C lamp.

3-3. Photocatalytic Stability of $TiO_2$/SAC

The reuse of a photocatalyst is significantly important for its practical application in wastewater treatment. To evaluate the photocatalytic stability of $TiO_2$/SAC, five cycle repeat experiments were carried out with 50 mg/L MO concentration, 30 g/L photocatalyst, and 48 h UV irradiation for cycling run. After the first photocatalytic reaction, the remaining solution was replaced with fresh MO solution of 50 mg/L, and $TiO_2$/SAC was reused without any treatment for the next cycles. As shown in Fig. 7, the degradation efficiency of MO decreased as repeated use times of $TiO_2$/SAC increased. After five cycles, the degradation efficiency of MO was 60%. This indicates that $TiO_2$/SAC still possesses relatively good photocatalytic activity. TOC removal with irradiation time was also investigated. As shown in Fig. 8, TOC removal decreased with increasing irradiation time. At the second cycle, 58% of the initial TOC was removed after photocatalytic reaction of 48 h. The efficiency of TOC removal in the five cycles was similar to that of the second cycle. Photocatalytic reaction of MO by $TiO_2$/SAC showed relatively high efficiency for TOC removal.

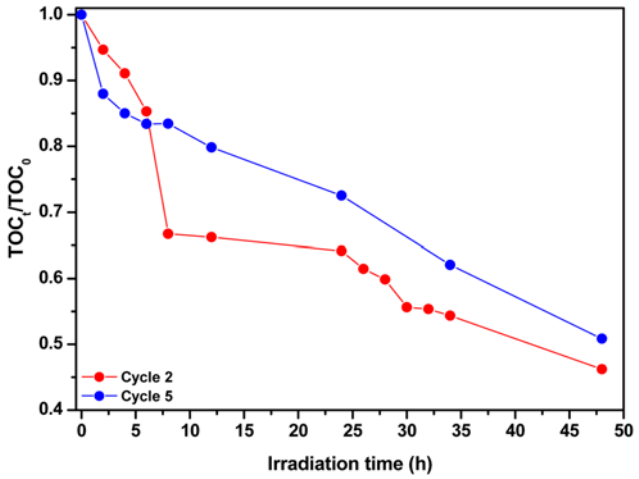


**Fig. 8. TOC removal during MO degradation by repeated use of $TiO_2$/SAC under UV irradiation (MO initial concentration: 50 mg/L, photocatalyst dosage: 30 g/L, pH 5.7, light source: UV-C lamp).**

3-4. Degradation Products of MO by $TiO_2$/SAC

Fig. 9 shows the change in UV-vis spectra of MO during photocatalytic reaction. The peak of MO at the maximum absorbance wavelength (468 nm) decreased and was slightly shifted to short wavelength at increasing irradiation time. The hypsochromic shift of the maximum absorption wavelength observed in the UV-vis spectra, as displayed in Fig. 9, may have occurred due to an *N*-demethylation process [40].

By being irradiated with light energy greater than its band gap energy, $TiO_2$ are producing electron and hole in the conduction band

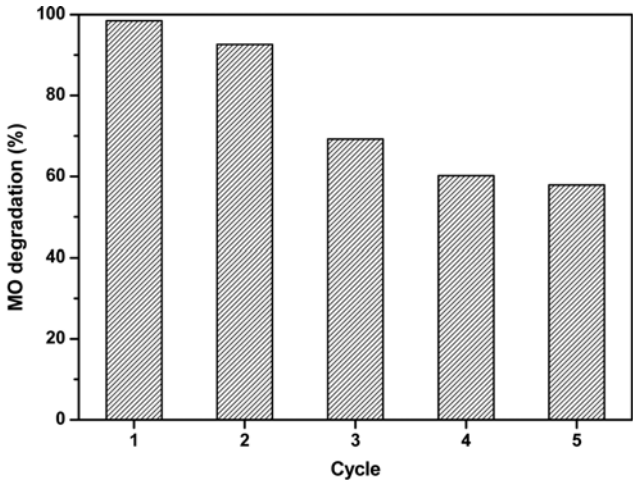


**Fig. 7. Photocatalytic efficiency of MO degradation by repeated use of $TiO_2$/SAC (MO initial concentration: 50 mg/L, photocatalyst dosage: 30 g/L, pH 5.7, light source: UV-C lamp, irradiation time: 48 h).**

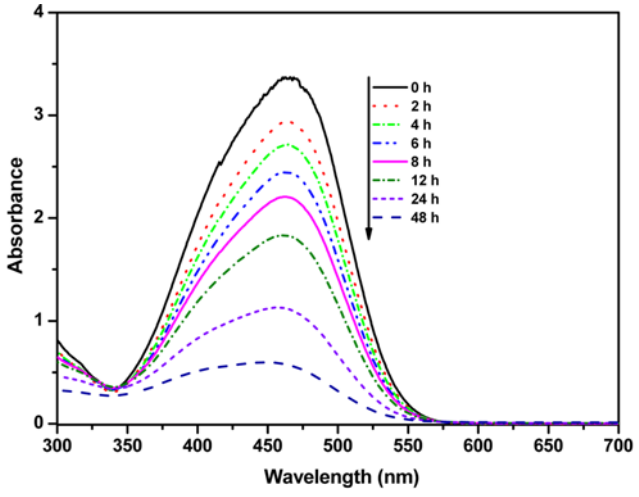


**Fig. 9. Variation of the UV-vis spectra of MO in aqueous solutions with increasing irradiation time (MO initial concentration: 50 mg/L, photocatalyst dosage: 30 g/L, pH 5.7, light source: UV-C lamp).**

and valance band, respectively. In the reaction of electron and hole, hydroxyl radical and superoxide radical, which are oxidizing reagents, generated by $H_2O$ and $O_2$ on the surface of $TiO_2$, decomposed the MO. The basic steps of photocatalytic reaction are as follows [2,5, 9,41-43]:

$$TiO_2+hv \rightarrow e^- (CB)+h^+ (VB) \quad (4)$$

$$e^- (CB)+O_2 \rightarrow O_2\cdot^- \quad (5)$$

$$h^+ (VB)+H_2O \rightarrow HO\cdot+H^+ \quad (6)$$

$$h^+ (VB)+OH^- \rightarrow HO\cdot \quad (7)$$

$$MO+HO\cdot \rightarrow \text{degradation products} \quad (8)$$

$$MO+\cdot O_2^- \rightarrow \text{degradation products} \quad (9)$$

To identify the degradation products of MO by $TiO_2$/SAC, LC/MS was analyzed. Fig. 10 shows a chromatogram of MO and sample after photocatalytic reaction of 24 h. As shown in Fig. 10(a), the peak of MO showed in the retention time of 8.7 min. After 24 h photocatalytic reaction, new peaks appeared at different retention time. Fig. 10(b) is the mass spectra of each retention time. The peak observed at retention time of 5.1 min is 4-((4-(methylamino)phenyl)diazenyl)benzenesulfonate and benzenesulfonate having m/z values at 290 and 156, respectively. The peak observed at retention time of 4.1 min is 4-((4-aminophenyl)diazenyl)benzenesulfonate and benzenesulfonate having m/z values at 276 and 156, respectively. Therefore, we inferred that the *N*-demethylation and part destruction of MO structure took place in the present system [44-47]. The peak of MO slightly decreased with increasing photocatalytic reaction, and the peak of degradation products observed at retention time of 5.1 min and 4.1 min increased and then decreased. This indicates that degradation products were decomposed into more small molecular intermediates with increasing irradiation time. Small molecular intermediates might not be detected by LC/MS analysis due to low concentration of solution or adsorption of small molecular intermediates on $TiO_2$/SAC. From the LC/MS spectrum, the degrada-

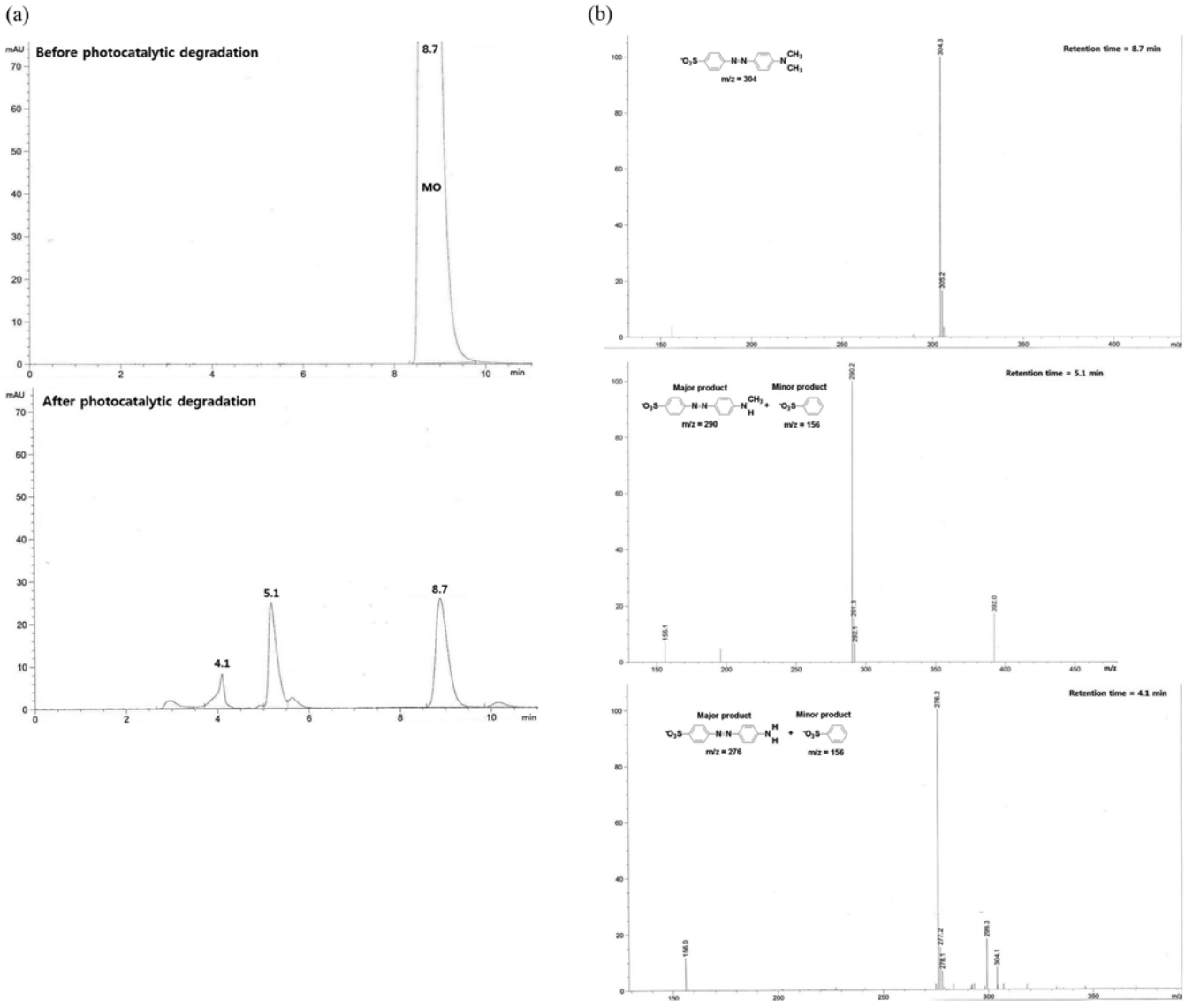


**Fig. 10. (a) Chromatogram of samples before and after photocatalytic degradation, (b) mass spectra of MO and degradation products (MO initial concentration: 50 mg/L, photocatalyst dosage: 30 g/L, pH 5.7, light source: UV-C lamp).**

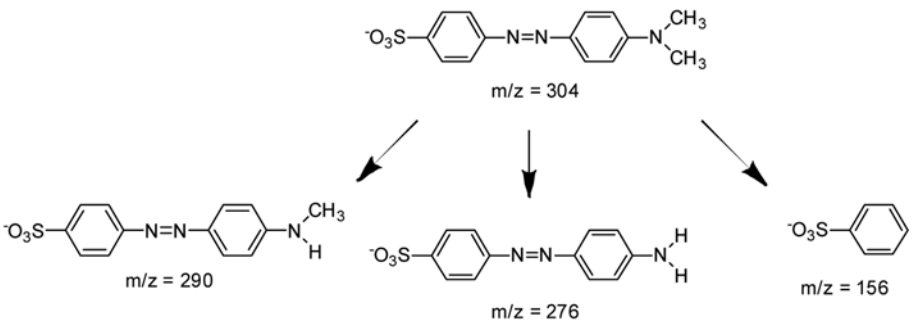


**Fig. 11. Possible degradation products of MO on the photocatalysis using $TiO_2$/SAC, as determined by LC/MS spectrum.**

tion products of MO by $TiO_2$/SAC are proposed in Fig. 11 [44,45].

## CONCLUSIONS

$TiO_2$ supported on spherical activated carbon was prepared via stabilization, carbonization, and activation process after ion-exchange reaction. Prepared $TiO_2$/SAC was used for adsorption and photocatalytic degradation of azo dye MO. The specific surface area of $TiO_2$/SAC, which has smooth spherical shape with diameter of 0.37-0.59 mm, was 458 $m^2$/g. From the XRD analysis, $TiO_2$ supported on spherical activated carbon was a mixture of anatase and rutile in the weight ratio 8 : 2. MO (50 mg/L) adsorption on $TiO_2$/SAC (5-30 g/L) quickly occurred within 1 h and reached almost equilibrium in about 3 h. $TiO_2$/SAC used in this study showed better photocatalytic activity in the range of 100-280 nm ($\lambda_{max}$=254 nm) compared to that of the range of 315-400 nm ($\lambda_{max}$=365 nm). The highest removal efficiency (98%) was observed for MO under experimental conditions for photocatalyst dosage of 30 g/L, an initial MO concentration of 50 mg/L, and an initial solution pH of 5.7, when the UV-C lamp was used as the light source. The photocatalytic degradation of MO by $TiO_2$/SAC in the presence of UV light was slowly performed compared to commercially available P25 $TiO_2$, but a maximum degradation efficiency of MO by $TiO_2$/SAC was same that of P25 $TiO_2$. Moreover, powder type as P25 $TiO_2$ requires an additional process step for separation of photocatalyst from treated water after photocatalysis. On the other hand, $TiO_2$/SAC used in this study does not need a separation process. The test for repeated use in five cycles indicated relatively good photocatalytic stability of $TiO_2$/SAC. Thus, $TiO_2$ supported on spherical activated carbon may be a possible application as an economic photocatalyst in practical dye wastewater treatment. The degradation products of MO in the presence of $TiO_2$/SAC under UV irradiation were proposed by LC/MS analysis. UV-vis spectra and LC/MS analysis indicated the methylation, demethylation, and breakup of the N=N bonds in this reaction system.

## ACKNOWLEDGEMENTS

This work is supported by Korea Ministry of Environment as "Converging technology project." The authors greatly appreciate this support.

## REFERENCES

1. N. M. Mahmoodi, M. Arami, N. Y. Limaee and N. S. Tabrizi, *Chem. Eng. J.*, **112**, 191 (2005).
2. I. K. Konstantinou and T. A. Albanis, *Appl. Catal. B.*, **49**, 1 (2004).
3. M. A. Rauf, M. A. Meetani and S. Hisaindee, *Desalination*, **276**, 13 (2011).
4. J. Guo, D. Jiang, Y. Wu, P. Zhou and Y. Lan, *J. Hazard. Mater.*, **194**, 290 (2011).
5. P. Jantawasu, T. Sreethawong and S. Chavadej, *Chem. Eng. J.*, **155**, 223 (2009).
6. R. G. Saratale, G. D. Saratale, J. S. Chang and S. P. Govindwar, *J. Taiwan Institute Chem. Eng.*, **42**, 138 (2011).
7. C. M. So, M. Y. Cheng, J. C. Yu and P. K. Wong, *Chemosphere*, **46**, 905 (2002).
8. S. Papić, N. Koprivanac, A. L. Božić and A. Meteš, *Dyes Pigm.*, **62**, 291 (2004).
9. H. Zhu, R. Jiang, L. Xiao, Y. Chang, Y. Guan, X. Li and G. Zeng, *J. Hazard. Mater.*, **169**, 933 (2009).
10. S. Wang and S. Zhou, *J. Hazard. Mater.*, **185**, 77 (2011).
11. X. Wang, Y. Liu, Z. Hu, Y. Chen, W. Liu and G. Zhao, *J. Hazard. Mater.*, **169**, 1061 (2009).
12. P. S. Yap, T. T. Lim and M. Srinivasan, *Catal. Today*, **161**, 46 (2011).
13. B. Tryba, A. W. Morawski and M. Inagaki, *Appl. Catal. B.*, **41**, 427 (2003).
14. X. Z. Li and H. Liu, *Environ. Sci. Technol.*, **37**, 3989 (2003).
15. W. Zhang, Y. Li, C. Wang and P. Wang, *Desalination*, **266**, 40 (2011).
16. S. X. Liu, X. Y. Chen and X. Chen, *J. Hazard. Mater.*, **143**, 257 (2007).
17. X. Wang, Z. Hu, Y. Chen, G. Zhao, Y. Liu and Z. Wen, *Appl. Surf. Sci.*, **255**, 3953 (2009).
18. B. Gao, P. S. Yap, T. M. Lim and T. T. Lim, *Chem. Eng. J.*, **171**, 1098 (2011).
19. J. Sun, X. Wang, J. Sun, R. Sun, S. Sun and L. Qiao, *J. Mol. Catal. A*, **260**, 241 (2006).
20. A. Y. Shan, T. I. M. Ghazi and S. A. Rashid, *Appl. Catal. A*, **389**, 1 (2010).
21. X. Zhang, M. Zhou and L. Lei, *Carbon*, **44**, 325 (2006).
22. H. J. Jung, MS Thesis, Chungnam National University, Korea (2008).
23. J. J. Lee, J. K. Suh, J. S. Hong, J. W. Park and J. M. Lee, *Korean Chem. Eng. Res.*, **44**, 375 (2006).
24. J. J. Lee, J. K. Suh, J. S. Hong, J. M. Lee and J. W. Park, *Mater. Sci. Forum*, **569**, 37 (2008).
25. J. J. Lee, J. K. Suh, J. S. Hong, J. M. Lee, Y. S. Lee and J. W. Park, *Carbon*, **46**, 1648 (2008).
26. J. J. Lee, J. K. Suh, J. S. Hong, J. M. Lee and J. W. Park, *Res. Chem.*

*Intermed.*, **35**, 337 (2009).
27. W. C. Jung, J. S. Hong, J. K. Suh and D. H. Suh, *Appl. Chem. Eng.*, **21**, 445 (2010).
28. H. J. Jung, J. S. Hong and J. K. Suh, *Korean J. Chem. Eng.*, **28**, 1882 (2011).
29. C. Karunakaran, G. Abiramasundari, P. Gomathisankar, G. Manikandan and V. Anandi, *J. Colloid Interface Sci.*, **352**, 68 (2010).
30. J. W. Shi, *Chem. Eng. J.*, **151**, 241 (2009).
31. M. Huang, C. Xu, Z. Wu, Y. Huang, J. Lin and J. Wu, *Dyes Pigm.*, **77**, 327 (2008).
32. S. H. Lin, C. H. Chiou, C. K. Chang and R. S. Juang, *J. Environ. Manage.*, **92**, 3098 (2011).
33. R. J. Tayade, T. S. Natarajan and H. C. Bajaj, *Ind. Eng. Chem. Res.*, **48**, 10262 (2009).
34. C. H. Wu and J. M. Chern, *Ind. Eng. Chem. Res.*, **45**, 6450 (2006).
35. C. Chen and C. Lu, *J. Phys. Chem. C*, **111**, 13922 (2007).
36. H. M. Coleman, V. Vimonses, G. Leslie and R. Amal, *J. Hazard. Mater.*, **146**, 496 (2007).
37. L. F. Velasco, J. B. Parra and C. O. Ania, *Appl. Surf. Sci.*, **256**, 5254 (2010).
38. Y. Li, S. Zhang, Q. Yu and W. Yin, *Appl. Surf. Sci.*, **253**, 9254 (2007).
39. X. Lin, F. Huang, W. Wang, Z. Shan and J. Shi, *Dyes Pigm.*, **78**, 39 (2008).
40. Y. Liu, Y. Ohko, R. Zhang, Y. Yang and Z. Zhang, *J. Hazard. Mater.*, **184**, 386 (2010).
41. S. Qourzal, M. Tamimi, A. Assabbane and Y. Ait-Ichou, *M. J. Condensed Matter*, **11**, 55 (2009).
42. P. Bansal, D. Singh and D. Sud, *Sep. Purif. Technol.*, **72**, 357 (2010).
43. M. N. Chong, B. Jin, C. W. K. Chowand and C. Saint, *Water Res.*, **44**, 2997 (2010).
44. K. Dai, H. Chen, T. Peng, D. Ke and H. Yi, *Chemosphere*, **69**, 1361 (2007).
45. T. Chen, Y. Zheng, J. M. Lin and G. Chen, *J. Am. Soc. Mass Spectrom.*, **19**, 997 (2008).
46. X. Z. Wu, M. Lingyue and K. Akiyama, *Luminescence*, **20**, 36 (2005).
47. C. Baiocchi, M. C. Brussino, E. Pramauro, A. B. Prevot, L. Palmisano and G. Marcì, *Int. J. Mass Spectrom.*, **214**, 247 (2002).